

## Numerical Simulation of 2D Separated Flows Using Two Different Turbulence Models

E. E. Elhadi, Lei Xiaosong and Wu Keqi

School of Energy and Power Engineering, Huazhong University of Science and Technology  
Wuhan, 430074, China

**Abstract:** The Navier Stock equations coupled, firstly with the standard k-ε turbulence model, secondly with Wilcox K-ω model were solved to study the phenomena of turbulent flow separation in different aeronautical and fluid mechanical applications. The numerical simulation based on modified SIMPLE algorithm was employed to non staggered grids which are constructed by using mid-point principle and gradient correction in Cartesian coordinates. Also the momentum interpolation scheme postulated by Pric was used to avoid pressure fluctuation. This numerical simulation was employed to simulate the turbulent flow past an airfoil with trailing edge separation and flow through sudden expansion pipe. In order to compare the results obtained by the two turbulence models, the predicted results by each model were compared with those of available experimental results and it was found out that Wilcox K-ω model is more accurate than k-ε model.

**Key Words:** Turbulent, Separation Flow, k-ε Turbulence Model, Wilcox K-ω Model, Airfoil, CFD

### Introduction

The study of flow separation from the surface of a solid body, and the determination of different changes in flow field that develop as a result of the separation, are among the most fundamental and difficult problems of fluid dynamics. In fact most liquid and gas flows encountered in engineering applications involve separation. Separation causes a considerable limitation on the operating characteristics of airfoils, turbomachinery blades, jet engines, rocket nozzles, etc., leading to significant effects on their performance. The problem of boundary layer separation is an old but still it has attracted considerable interest amongst researchers. In order to calculate fluid flows with turbulent boundary layer separation in engineering, it is often necessary to select the suitable turbulence model. Bradshaw (1972) stated that "A numerical procedure without a turbulence closure model stands in the same relation to a complete calculation method as an ox does to bull". Johnson and King (1985) developed turbulence closure model for two dimensional, turbulent boundary layer flows subjected to serve adverse pressure gradients. Rodi (1982) introduced briefly the merits and demerits of different types of turbulence models. Rhie and Chow (1983) used finite volume numerical method to solve incompressible, steady Navier Stock equations in general curvilinear coordinates coupled by k-ε turbulent model to analyze the turbulent flow a round the airfoil with and without trailing edge separation. Rodrick and Chima (1995) developed two equations K-ω turbulence model and he applied these two equations to a quasi-three-dimensional viscous analysis code for blade-to-blade flows in turbomachinery. Roger *et al.*, (1981) made experimental works which are very useful in understanding the structure of separating turbulent boundary layer, he predicted a very useful turbulence correlations.

This work aims to develop a numerical simulation to study and analyze the 2-D separated flow which occurs in many aeronautical and fluid mechanical applications

and to compare the accuracy of k-ε turbulence model with that of Wilcox K-ω turbulence model.

**Numerical Simulation:** The numerical simulations in this work are based on coupling the Navier stock equations firstly with k-ε turbulence model and secondly with K-ω Turbulence model. The basic equations and relations which are used in these simulations are illustrated as follows:-

**Govern Equations and Turbulence Models:** Steady, incompressible Navier stoke equations based on the Boussinesq approximation were employed in the following form

$$\frac{\partial}{\partial x_i}(\rho u_i) = 0.0 \quad (1)$$

$$\frac{\partial}{\partial x_j}(\rho u_i u_j) = -\frac{\partial p}{\partial x_i} + \frac{\partial}{\partial x_j}(\mu + \mu_t)\left(\frac{\partial u_i}{\partial x_j} + \frac{\partial u_j}{\partial x_i}\right) - \frac{2}{3}\delta_{ij}\rho K \quad (2)$$

In order to close the N-S equations, an approximate turbulence model should be employed. In this paper, two different turbulent models (k-ε and K-ω) were employed separately for the purpose of comparing between them. The govern equations of turbulence model in general form are:

$$\mu_t = \mu_t(z_1, z_2) \quad (3)$$

$$\frac{\partial}{\partial x_i}(\rho u_i z_m) = \frac{\partial}{\partial x_i}\left[\left(\mu + \frac{\mu_t}{\sigma_{z_m}}\right)\frac{\partial z_m}{\partial x_i}\right] + s_{z_m} \quad (4)$$

The different properties and empirical constants in Eq.3 and Eq.4 (Rhie and Chow, 1983 and Rodrick and Chima, 1995) for:

(i) K-ε model are

$$m = 1 \text{ or } 2 \quad z_1 = K \quad z_2 = \varepsilon = \beta^* \omega K$$

$$\mu_t = \mu \frac{\rho K^2}{\varepsilon} \quad s_k = c_\mu \rho K^2 \frac{\Phi}{\varepsilon} - \rho \varepsilon$$

$$s_\varepsilon = c_1 c_\mu \rho K \Phi - c_2 \rho \frac{\varepsilon^2}{K}$$

$$c_1 = 1.44 \quad c_2 = 1.92 \quad c_\mu = 0.09$$

$$\sigma_k = 1.0 \quad \sigma_\varepsilon = 1.3 \quad \beta^* = 0.09$$

(ii) K- $\omega$  model are

$$m = 1 \text{ or } 2 \quad z_1 = K \quad z_2 = \omega = \frac{\epsilon}{\beta^* K}$$

$$\mu_t = \frac{\gamma^* \rho K}{\epsilon} \quad s_k = \frac{\gamma^* \rho K}{\omega} - \beta^* \rho \omega K$$

$$s_\epsilon = \gamma \gamma^* \rho \Phi - \beta \rho \omega^2$$

$$\gamma^* = 1.00 \quad \gamma = \frac{5}{9} \quad \beta^* = 0.09$$

$$\beta = \frac{3}{40} \quad \sigma_k = 2.0 \quad \sigma_\epsilon = 2.0$$

$$\Phi = \frac{\partial u_i}{\partial x_j} \left( \frac{\partial u_i}{\partial x_j} + \frac{\partial u_j}{\partial x_i} \right) \quad (5)$$

**Discretization of Govern Equations:** In the present work non staggered grids were used. These grids were constructed by using mid-point principle and gradient correction in Cartesian coordinates. Also the momentum interpolation scheme postulated by Peric (1988) was used to avoid pressure fluctuations.

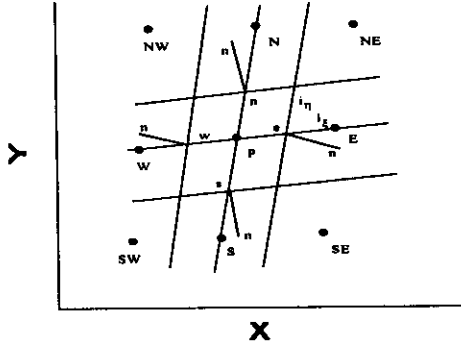


Fig.1: Sample of Grid Representation

Integrate (1) and (2) for control volume (Fig.1) yields

$$F_e - F_w + F_n - F_s = R \quad (6)$$

F's terms are evaluated differently for mass and momentum conservation. In case of continuity equation

$$F_e = m_e = \rho_e (S^x u_x + S^y u_y)_e \quad (7)$$

In case of momentum equation F contains two terms which are:

$$F_e^c = \rho_e (S^x \phi_x + S^y \phi_y) (\phi_i)_e \quad (8)$$

$$F_e^d = \mu_e S_e \frac{(\phi_i)_e - (\phi_i)_p}{dis(PE)} + \mu_e S_e \overline{(grad \phi_i)_e} (n - i_\epsilon) \quad (9)$$

Similar expressions as these in Eq. 6 to Eq. 9 can be written for other faces n, s, w. over bar indicates that, linear interpolation is used and  $\phi$  refer to velocity components and  $(\phi_i)_e$  is given by Majumar (1988) as follows

$$(\phi_i)_e = \phi_p \cdot f + \phi_E (1 - f) \quad (10)$$

geometric interpolation factor f is given by

$$f = \frac{dis(eE)}{dis(PE)}$$

Discretized momentum equation can be arranged in the following form:

$$A_\phi \phi^p + \sum_{l=N,S,E,W} A_l \phi_l = S^\phi \quad (11)$$

$$A_l = \begin{cases} (-\frac{(vS)_l}{dis(Pl)}) - \min(m_l, 0) & l = N, E \\ (-\frac{(vS)_l}{dis(Pl)}) + \min(m_l, 0) & l = S, W \end{cases}$$

$$A_\phi = - \sum_{l=N,S,E,W} A_l$$

$$S^\phi = \sum_{l=N,S,E,W} F_d^{\phi,e} - F_d^{\phi,i} + F_C^{\phi,i} - F_C^{\phi,i} + P^\phi$$

#### Coupling Pressure and Velocity and Pressure Correction Method:

In order to obtain a pressure and velocity fields that satisfy the mass and momentum conservation laws a modified SIMPLE method is used. In this modified method to avoid the existence of the pressure fluctuations, the pressure correction equation is reconstructed to supply information of pressure at point p (Fig.1). These are done through following relations.

$$\phi_e = \bar{\phi}_e - \Delta \Omega_e \left( \frac{1}{A_p^\phi} \right)_e \left( \left( \frac{\partial p}{\partial x} \right)_e - \overline{\left( \frac{\partial p}{\partial x} \right)_e} \right) \quad (12)$$

where

$$\left( \frac{\partial p}{\partial x} \right)_e \approx \frac{P_E - P_P}{\Delta x} \quad \Delta \Omega_e = (x_E - x_P) \Delta y$$

$$\left( \frac{1}{A_p^\phi} \right)_e = \frac{1}{\Delta \Omega_e} \left( \frac{(1-f_1)\Omega_P}{A_P^\phi} + \frac{f_1 \Omega_E}{A_E^\phi} \right) \quad f_1 = \frac{x_E - x_P}{x_E - x_P}$$

Eq. 12 indicates that if the pressure is known the velocity components can be calculated by using this equation. In the present paper, initial guess of the pressure field is assumed ( $P^{m-1}$ ) and Eq. 12 is used to

calculate the velocity components ( $\phi^{m*}$ ). The guessed

pressure is corrected ( $P^m$ ) until the resulting velocity satisfy the continuity equation. The relations used to correct the guessed pressure and hence velocity field ( $\phi$ ) are:

$$\phi_{i,p}^{m*} = \frac{(1-\alpha_\phi) \phi_p^{m-1} - \sum_{l=N,S,E,W} A_l^\phi \phi_l^{m*}}{A_p^\phi} - \frac{1}{A_p^\phi} \left( \frac{\partial P^{m-1}}{\partial x_i} \right)_p \quad (13)$$

$$\phi_i^m = \phi_i^{m*} + \phi_i' \quad (14)$$

$$P^m = P^{m-1} + P' \quad (15)$$

$$\phi_{i,p}^m = \tilde{\phi}_{i,p}^m - \frac{1}{A_p^\phi} \left( \frac{\partial P^m}{\partial x_i} \right)_p \quad (16)$$

$$\phi_{i,p}' \cong -\frac{1}{A_p^\phi} \left( \frac{\partial P'}{\partial x_i} \right)_p \quad (17)$$

$$m_e \approx -(\rho \Delta \Omega S)_e \left( \frac{1}{A_p^\phi} \right)_e \frac{P_E' - P_P'}{dis(PE)} \quad (18)$$

In similar manner Eq. 12 and Eq. 18 can be applied to other faces (n, m, s). Finally discretized equation for

correction pressure ( $P'$ ) is derived in the following form

$$A_p P' + \sum_{l=E,W,N,S} A_l P_l' = S^P \quad (19)$$

Where

$$A_l = \frac{1}{2} \rho \left( \frac{\Omega_p}{A_p} + \frac{\Omega_l}{A_l} \right) \frac{S_l}{\xi_{l,n}} \quad \text{here } \Omega \text{ for pressure}$$

$$A_p = - \sum_{l=n,s,e,w} A_l \quad S^P = \sum_{l=n,s,e,w} m_l$$

**Boundary Conditions:** In order to apply the present numerical simulations to internal and external flows, the following boundary conditions are considered.

**Inlet Boundary Conditions:** Inlet boundary conditions are defined as

$$\text{For velocity } u_{j,in} = u_j(x, y) \quad j=1,2$$

For turbulence model

$$K_{in} = \frac{\sum_{j=1,2} u_j^2}{200}$$

$$\varepsilon_{in} = C_\mu K_{in}^{\frac{3}{2}} / 0.03L$$

$$\omega_{in} = \frac{\rho K_{in}}{\mu_t}$$

The velocity  $u$  and characteristic length  $L$  must be defined as input data.

**Outlet Boundary Conditions:**

$$\frac{\partial u_j}{\partial n} = \frac{\partial K}{\partial n} = \frac{\partial \varepsilon}{\partial n} = \frac{\partial \omega}{\partial n} = 0.0$$

**On Solid Wall:** For no slip condition  $u_j = 0.0$

For K- $\omega$  turbulence model

$$K = 0.0$$

$$\omega = \frac{\mu_t^2}{\gamma} S_R = S_R \left( \frac{\partial u}{\partial y} \right)_{wall}$$

for k- $\varepsilon$  turbulence model

$$\varepsilon = C_\mu^{\frac{3}{4}} \frac{K^{\frac{3}{2}}}{l}$$

$$l = 0.07L$$

$$\frac{\partial K}{\partial n} = 0.0$$

If  $y$  is the coordinate direction normal to the solid wall the turbulent kinematics viscosity ( $\nu_t$ ) at point  $y_p$  with

( $11.6 \leq y_p^+ \leq 400$ ) is given by

$$(\nu_t)_{wall} = \frac{y_p^+ \nu}{\left( \frac{1}{K} \ln y_p^+ + B \right)}$$

Non dimensional boundary layer coordinate  $y_p^+$  is given by

$$y_p^+ = \frac{y_p C_\mu^{\frac{1}{4}} K_p^{\frac{1}{2}}}{\rho \nu}$$

Where  $K$  and  $B$  are universal constants. But their values are 0.4 and 5.49 respectively.

**Free Stream Boundary Conditions:** These conditions are considered in the case of external flow which are  $u = U_\infty$

$$K = \varepsilon = \omega = 0.0$$

**Symmetry Boundary Conditions:**

$$V_n = 0.0$$

$$\frac{\partial \phi}{\partial n} = 0.0 \quad \phi = K, \varepsilon, \omega, \gamma, \text{ or } P$$

**Numerical Simulation Steps:**

1. Modified multiple grid method is used to generate non-staged grid arrangement. For more information about this method Thomposon *et al.*, (1985) and Majumdar (1988).
2. The pressure field obtained from initial guess or previous iteration ( $P^{n-1}$ ) is used to solve momentum equation 11 to find the velocity components. The discretized equations like Eq. 11 are solved by using SIP method suggested by Stone (1968).
3. The pressure correction Eq. 19 is solved. The pressure, velocity and mass flow rate are corrected by Eqs. 13-18.
4. solve the turbulence model Eqs. 3 - 4 for each of k- $\varepsilon$  and K- $\omega$  turbulence model.
5. The above steps (2 - 4) are repeated until these conditions

$$\sum \frac{|m_p|}{Q} < 10^{-4} \quad \text{and} \quad \frac{\max |m_p|}{Q}$$

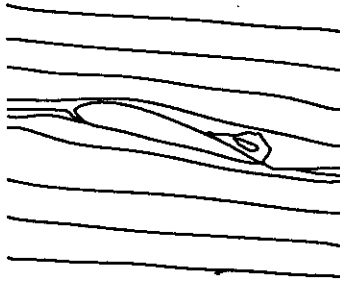
are satisfied. Summation is taken over all points and  $Q$  is inlet flow rate.

6. According to above steps a computer program coded "SEPA" is developed and used as a tool to analysis in this work. This code can be applied to internal and external flows, SEPA's users need only to input the geometric parameters of the selected 2D configuration, boundary conditions and initial grid.

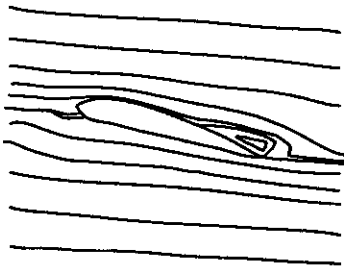
## Results and Discussion

The present numerical simulations are applied to analyze the internal and external flows. For the purpose of explanation and validation of the present work, two cases were considered which are flow over NACA 4412 airfoil and flow through sudden expansion pipe.

**Flow Over NACA 4412:** For the purpose of applying the present numerical simulations to external flow, the flow past NACA 4412 airfoil at maximum lift condition with a  $13.87^\circ$  angle of attack is calculated and the predicted results are shown in Fig.2 and Fig.3.

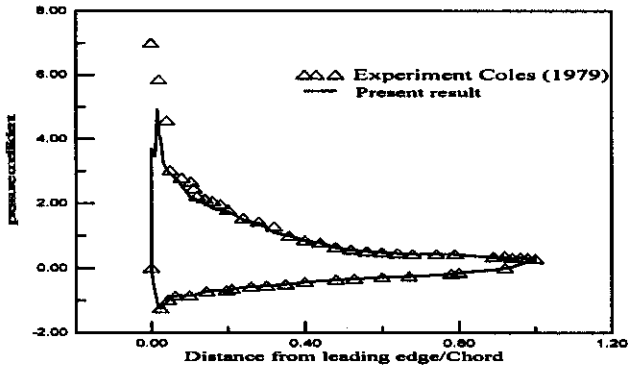


a. PREDICTED BY K -  $\epsilon$

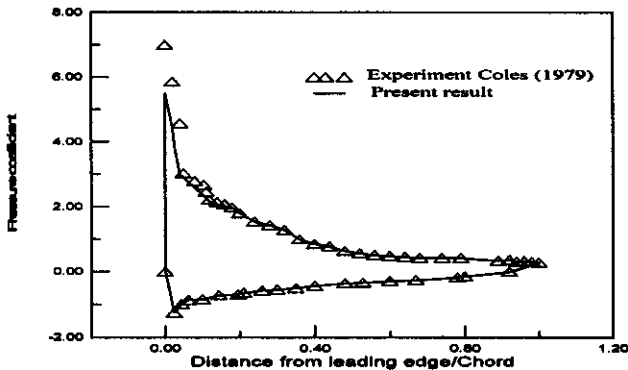


b. PREDICTED BY K -  $\omega$

Fig.2: Streamlines for NACA 4412 Airfoil at  $13.87^\circ$  Incidence ( $R_{re} = 1.5 \times 10^6$ )

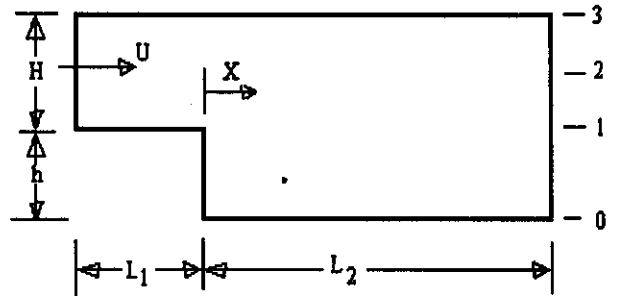


A. Predicted by K -  $\epsilon$  Model



B. Predicted by K -  $\omega$  Model

Fig. 3: Surface Pressure Distribution For NACA 4412 Airfoil At  $13.87^\circ$  Deg Incidence ( $R_{re} = 1.5 \times 10^6$ )



$$H=0.762 \text{ m} \quad h=0.0381 \text{ m} \quad L_1=0.1524 \text{ m}$$

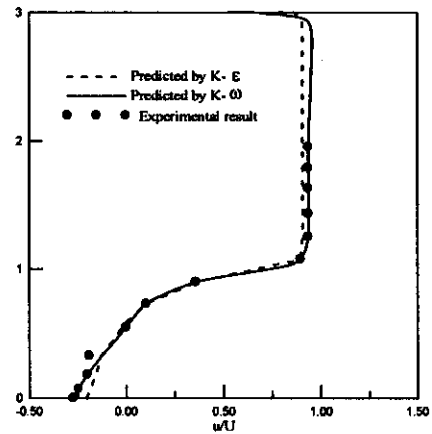
$$L_2=2.3388 \text{ m}$$

$$\rho = 1.88553 \text{ Kg/m}^3$$

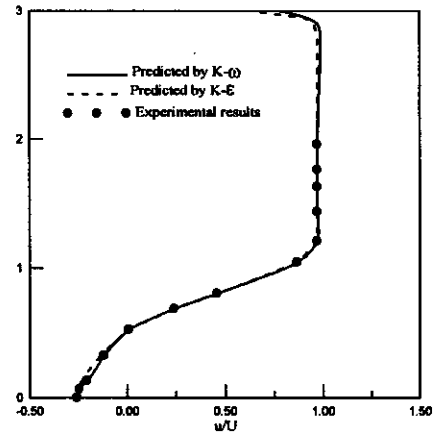
$$\mu = 1.83698 \times 10^{-5} \text{ Kg/m.sec}$$

$$U=17.8 \text{ m/sec}$$

Fig. 4: Sudden Expansion Pipe



a. AT  $X/h = 1.333$



b. AT  $X/h = 2.667$

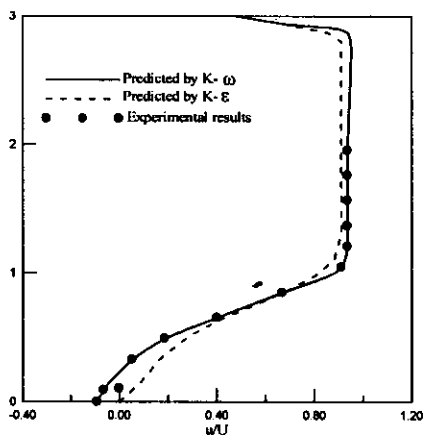
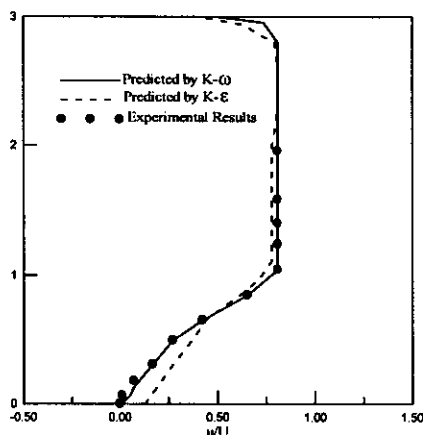
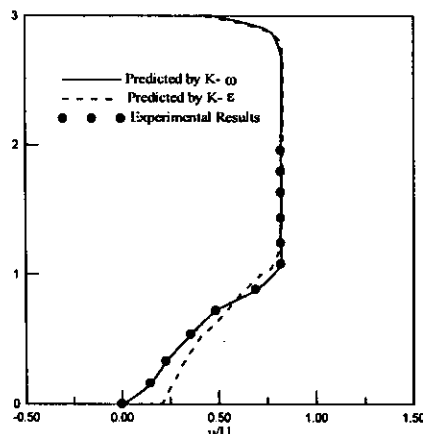

c. AT  $X/h = 5.333$ 

d. AT  $X/h = 7.113$ 

e. AT  $X/h = 8$ 

Fig. 5: Sudden Expansion Pipe Velocity Profile at Different Axial Locations

Fig. 2 shows the streamlines flow pattern which are predicted by the present numerical simulation. It is clearly seen from Fig.2 that, the trailing edge separation bubble which predicted by using  $K-\omega$  turbulence model is more clear and more effective on the free streamlines than predicted by the  $K-\epsilon$  turbulence model.

As shown in Fig. 3 that, good agreement between the surface pressure distribution which is calculated by using  $K-\omega$  model and experimental results. Also it is seen from Fig. 3.a that,  $K-\epsilon$  model fails in predicting the pressure near the leading edge of airfoil, at this region the pressure reaches it's peak value.

**Flow Through Sudden Expansion Pipe:** For the purpose of applying the present numerical simulations to internal flow, the flow in sudden expansion circular pipe was analyzed by using the present simulation. The geometric constructions of it and flow properties are shown in Fig. 4

Fig. 5 shows the sudden expansion pipe velocity profile at different axial locations. As shown in Fig. 4 y-axis is divided into three regions. Measurement (Peric et al., 1988 and Menter 1992) were taken in regions 0-1 and 1-2. it can be observed from these figures that, there is a good agreement between results predicted by  $K-\omega$  model and that predicted by experiments. It is clearly seen that, flow reattaches at axial location  $X = 7.113h$ . At this axial location the results predicted by  $K-\epsilon$  model differ from that predicted by experiments which indicates that  $K-\omega$  model is more accurate than  $K-\epsilon$  model especially in these critical regions. Also after reattachment there is still a good agreement between experiment results and that calculated using  $K-\omega$  turbulence model.

## Conclusion

A new numerical simulation has been developed for two-dimensional turbulent boundary layers with separated flow using two different turbulence models. Based on comparison of the experiments for flow past NACA 4412 airfoil and flow through sudden expansion pipe, numerical simulations indicate that,  $K-\omega$  turbulence model has following advantages over  $K-\epsilon$  turbulence model:

- $K-\omega$  turbulence model behaves well numerically.
- $K-\omega$  turbulence model has high performance especially in a variety of important regions such as fully developed flow in case of sudden expansion pipe, high pressure regions in case of leading edge of airfoil.
- $K-\omega$  turbulence model has high ability to predict most of the important phenomena which occur in separated regions.

## Nomenclature

|            |                           |
|------------|---------------------------|
| $u$        | velocity component        |
| $P$        | pressure                  |
| $K$        | turbulence kinetic energy |
| $S_e$      | face e area               |
| $U_\infty$ | free stream velocity      |
| $n$        | unit vector               |

$m$  mass flow rate

$m_e$  corrected mass flow rate through face e

$R$  residual of integral

## Elhadi et al.,: Numerical Simulation of 2D-Separated Flows

|                |  |
|----------------|--|
| $R_{ec}$       | Reynold number based on airfoil chord    |
| $S^x, S^y$     | areas                                    |
| $x, y$         | Cartesian coordinates                    |
| $\varepsilon$  | turbulence kinetic energy dissipation    |
| $\alpha_u$     | under relaxation parameter ( $<1.0$ )    |
| $\bar{\phi}_e$ | linear average value of $\phi$ at face e |
| $\mu$          | laminar viscosity                        |
| $\mu_t$        | turbulent viscosity                      |
| $\rho$         | density                                  |
| $\nu$          | kinematics viscosity                     |
| $\delta_{ij}$  | Kronecker factor                         |
| $\omega$       | specific dissipation rate                |

### References

- Bradshaw, P., 1972. "The Understanding and Prediction of Turbulent Flow," *Aeronautical J.*, Vol.76, No. 739, 403-418.
- Coles, D. and A. J. Wad Cock, 1979. "Flying Hotwire Study of flow past NACA 4412 Airfoil at Maximum lift", *AIAA J.*, Vol.17, 321-329.
- Johnson, D. A. and L. S. King, 1985. "A mathematically Simple Turbulence Closure Model for Attached and Separated Turbulent Boundary Layers" *AIAA J.*, Vol. 23, No.11, 1684-1692.
- Majumdar, S., 1988. "Role of under Relaxation in momentum interpolation for calculation of flow with non staggered Grids", *Numerical Heat transfer*, Vol.13. 125-132.
- Menter, F. R., 1992. "Performance of Popular Turbulence model for attached and separated adverse pressure gradient flows", *AIAA J.*, Vol.30.
- Peric, M. R.; Kessler and Scheuerer, 1988. "Comparison of Finite volume Numerical Methods with Staggered and Colocated Grids", *Computers and Fluids*, vol.16, No. 4, 389-403.
- Rodi, W., 1982. "Examples of turbulence models for Incompressible Flows". *AIAA J.*, Vol. 20, No.7. 872-879.
- Rhie, C. M. and W. L. Chow, 1983. "Numerical study of the turbulent flow past Airfoil with trailing Edge Separation" *AIAA J.*, Vol.21, No.11, 1525-1532.
- Rodrick, V. and Chima, 1995. "A K Turbulence Model for Quasi-Three-Dimensional Turbomachinery Flows", *NACA Report*.
- Roger, L.; Simpson and Y. T. Chew, 1981. "The structure of a separating turbulent boundary layer. Part 1. Mean flow and Reynolds stress, *J. Fluid Mechanics*, vol. 113, 23-51.
- Shih, T. M. and A. L. Ren, 1984. "Primitive-Variable Formulations using Nonstaggered Grids", *Numerical Heat Transfer*, Vol. 7, 413-428.
- Stone, H. L., 1968. "Iterative Solution of Implicit Approximation of Multi-dimensional Partial Differential equations" *SIAM J. of Numerical Analysis*, vol.5, 530-538.
- Thomson, J. F.; Warsi and C. Mastin, 1985. "Numerical Grid Generation, Foundation and applications", North-Holland.
- Thomas, P. D. and J. F. Middlecoff, 1980. "Direct Control of The Grid Point Distribution in Meshes Generated by Elliptic Equations", *AIAA J.*, Vol. 18, No. 6, 652-656.